Determination of Defect Criticality and the Resulting Performance Effects of CFRP Strengthened RC Beams

Jason Delaney,Vistasp Karbhari
UC San Diego, San Diego, CA

The effectiveness of externally bonded Carbon Fiber Reinforced Polymer (CFRP) composites in structural rehabilitation is strongly dependent on the bond performance between the CFRP and the reinforced concrete surface to which it is bonded. Many recent studies have been conducted as an attempt to quantify aspects of bond performance and bond behavior in this situation. Due to the complexity of the problem, most research has been conducted only on idealized specimens. This study investigates how bond performance may be affected in less than ideal conditions involving specific defects that may be encountered in the field. Any defects in the FRP, concrete, or at the bond line may result in stress concentrations causing local bond failure and therefore may produce an unfavorable influence on the global strengthening performance. Large-scale flexural tests are utilized to investigate the bond behavior of precracked specimens involving various defects such as crack spacing, unbonded length, unbonded shape, unbonded location, and waviness in CFRP fiber orientation. From these tests it is hoped that the critical aspects of defects that have an adverse influence on the global strengthening performance of a rehabilitated section may be determined. The resulting data allows for crucial observations to be made pertaining to how to relate idealized or more "perfect" laboratory behavior to specific "imperfect" field applications.

INTRODUCTION

Behavior and modeling of FRP strengthened concrete flexural members has been a topic of interest for several years. Although it is generally understood that FRP strengthening can significantly increase structural stiffness and strength, models still need considerable work to optimize economy and effectiveness. In addition, the behavior of common defects found in the FRP strengthening process is not well understood and needs addressed further.

There are three constitutive elements in external FRP bonded strengthening of concrete structures: the FRP composite, the concrete substrate, and the adhesive bonding them together (Niu et al. 2005). Defects in any of the three constitutive materials may result in detrimental strengthening performance. In practical application some defects may be unavoidable, especially for in-service structures where conditions may be less than ideal. To date several studies may be found involving all aspects of defects in the FRP material ranging from very small to relatively large in scope (Navada. 2004). Most of these investigations have taken place in the auto or aerospace industries and assume somewhat different conditions and service requirements than are required for civil infrastructure. However, Navada (2004) has recently addressed many of

these issues. Since defects in the FRP have been given this attention thus far, this study focuses primarily on the effects of defects contained in the adhesive, the concrete substrate, and the implications involved when defective FRP are bonded to the concrete.

Background

To date, only a limited number of studies have been conducted involving FRP defects in civil infrastructure. In an effort to isolate performance impacts for modeling purposes these investigations were conducted primarily at the component level or with atypical loading scenarios, such that the failure modes were different from those in a practical structure. In reality, defects may not play the same critical role if tests are conducted at the structural level. Kaiser (2002) studied the effect of different defects in the application of wet lay-up of FRP to concrete using a fracture mechanics approach. A mixed-mode peel test was utilized to compare fracture energy release rates (FERR) to control specimens on the basis that the presence of defects in the bond between FRP and concrete can influence the resistance to debonding. The effects of damage to free edges, incorrect stoichiometry, inadequate primer, concrete cavities, and prolonged primer cure were tested to measure the corresponding detriment to FERR. Pertinent to this study, minor concrete cavities did not appear to be detrimental to fracture toughness due to an increase of the fracture path and the critical size of a circular disbond was found to be of a diameter half the width of the FRP. Similarly, Navada also used FERR in mixed-mode peel tests to investigate the impact of defects occurring in critical environments. Defects such as inadequate primer, excessive primer, substrate moisture, delaminations, and disbonds were subjected to various environments such as ambient conditions, heat, freeze, immersion, and ponding to determine changes in FERR. Additionally, Yang and Nanni et al. (2002) investigated the effects of fiber misalignment in tensile coupons and found that a deviation in fiber orientation as small as 5% can have a significant influence. Bizindavyi and Neale (1999), through single lap shear tests, suggested that cracking may increase stress transfer length. However, somewhat contradictory, Ueda (2002) suggested that cracks deteriorated bond response in FRP strengthened concrete members. More research is needed to clarify the impact of concrete cracking on FRP strengthening behavior. Additionally, more comprehensive models must be developed for application of future design and analysis.

EXPERIMENTAL PROGRAM

The experimental setup can be seen in Figure (1) below. Large-scale flexural tests are utilized for the purpose of assessing defect criticality and bond performance. This setup was chosen in order to model with confidence, the loading scenarios commonly encountered in the field. These tests were designed such that data can be collected both locally and globally to determine a defects influence on structural behavior. The results should allow for the formulation of “damage curves” to assess what impact such defects may have on an actual rehabilitated structure in the field. Upon completion, the testing program should provide data for use in modifying the current design standards to provide insight on the behavior of some of the most common and most critical defects.

Specimen Setup and Testing Details

The test setup is designed such that the head of the actuator applies the load directly through two elastomeric pads symmetrically about the midspan of the beam. This loading configuration was chosen so additional confining stresses at the mid-span of the beam are avoided, thus ensuring

that concrete crushing occurs close to its true compressive strength. The concrete specimens are two meters in length with cross sectional dimensions of 150mm x 200mm deep (Fig. 3). Longitudinal reinforcement consists of two 13mm (#4) bars, top and bottom, providing reinforcement to promote a ductile beam behavior. The transverse reinforcements are 10mm (#3) bars at 80 mm spacing. This spacing ensures that shear failure will not occur, but some shear cracking may still occur in the FRP strengthened specimens. The concrete used was ordered specified at 28 MPa (4000psi) with a resulting strength of 35 MPa (5100psi). The beams were designed such that a large ductility is provided such that a defect's affect can be observed in a consistent environment (i.e. known virgin beam strength at all given deflections).

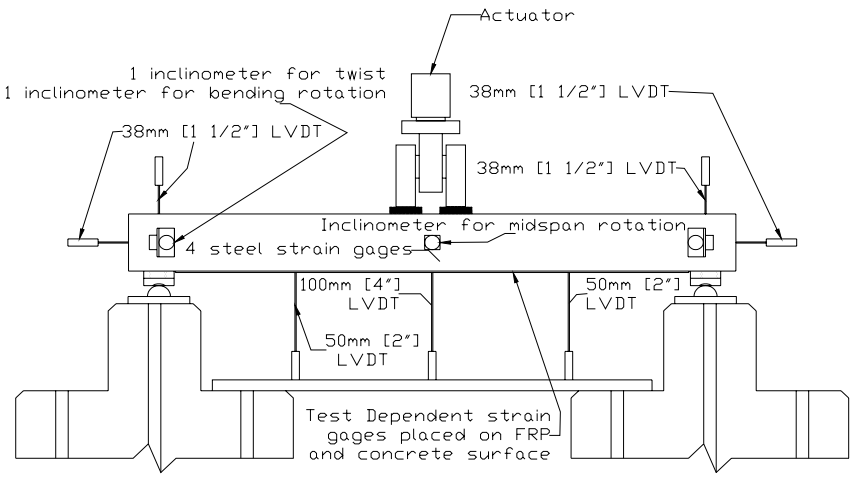

Figure 1: Instrumentation and test setup.

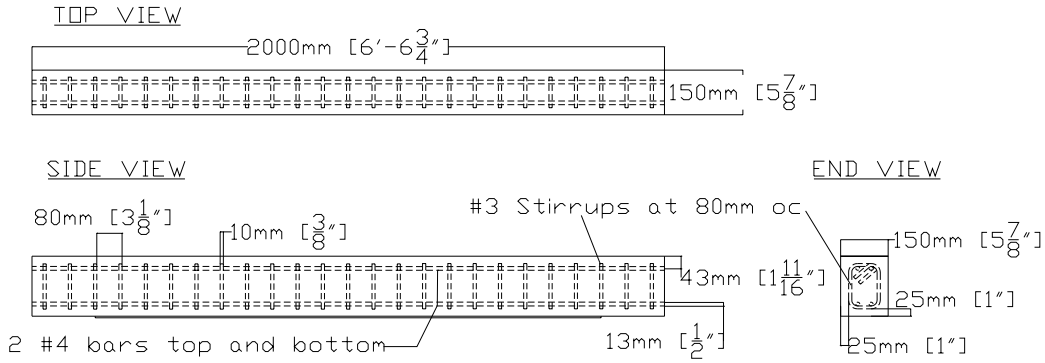

Figure 2: Specimen details.

The specimens were all outfitted with four strain gages on the longitudinal steel, two at the mid-span and one at each quarter point. The purpose behind these gages is primarily for usage in precracking and also to compare the steel behavior when testing various defects involving the FRP. Externally, one to three concrete strain gages are used to monitor concrete stresses and verify the plane sections assumption during testing and are applied at the beam's midspan. In addition, up to ten strain gages are strategically placed on the FRP surface of each specimen to

monitor the composites behavior at and around the defects. Finally, the key instrumentation for the purpose of monitoring global behavior is three LVDTs. One is utilized at the midspan to measure maximum structural displacement, while the other two are at the quarter-spans to monitor the specimens for irregular curvature. Additional instrumentation is also utilized, but primarily only to ensure the specimen is not twisting or sliding on the supports in an unexpected manner.

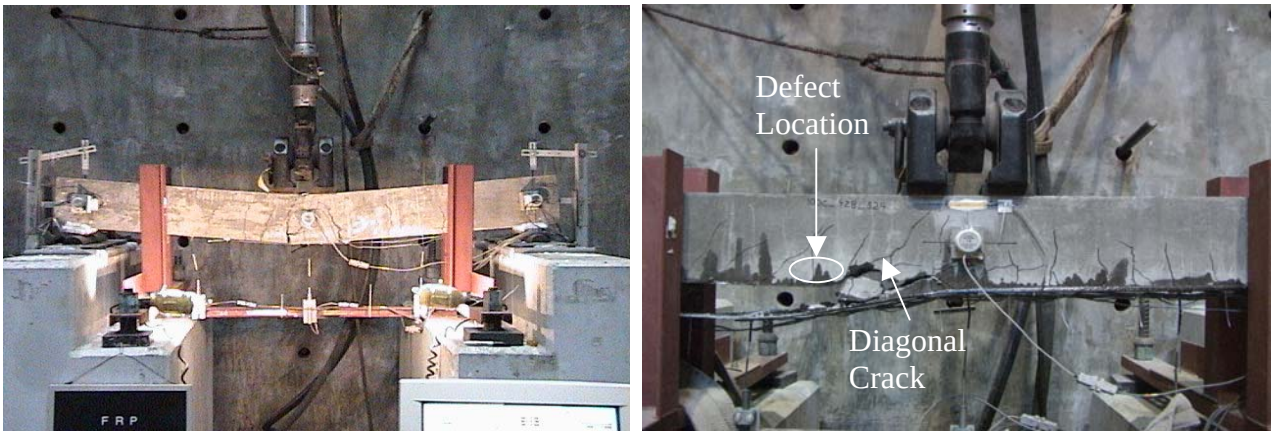

Figure 3: Left – failed control specimen. Right – failed specimen with disbond inserted.

The majority of the 62 specimens tested are preloaded to 8 kips load prior to the application of FRP. This preload corresponds to approximately 95% of yield and 85% of the maximum strength of an unstrengthened specimen and corresponds to a maximum concrete crack opening of about 0.25mm, the maximum allowable by NCHRP 514 (2004). This preloading causes damage in the specimen intended to simulate field conditions where damaged concrete is anticipated. The specimen is then unloaded and FRP is applied to the tension face, inserting a predetermined defect configuration. After curing, each specimen has strain gages applied to the FRP surface and are loaded to failure in approximately three to four increasing load cycles.

Defects Considered

Defects considered in this study include: disbonds at the concrete/FRP interface, disponds between FRP layers, excessive preload cracking, porous concrete, and FRP fiber misalignment. The Teflon disbonds were created using thin, flexible Teflon sheets in order to prevent bonding of the FRP. Various locations, shapes, and sizes of disbonds were assigned to the a specimen and repeated as deemed appropriate. Predictions using finite element modeling were utilized to determine initial sizes and locations of defects before testing began. Also, locations of defects were chosen based on the beam body forces at various points (e.g. high moment/high shear, high moment/low shear, or low moment/high shear regions). Excessive preload cracking will be examined by subjecting the specimens to a greater preload, causing increased crack opening and size as well as greater permanent deformations due to exceeding steel yielding. The condition of porous concrete can be encountered when the concrete is badly damaged by aging/chemicals or due to air entrapment against the form at the time it was cast. In the event that such porous regions are not properly filled with epoxy or some other appropriate filler, it would be beneficial to know whether the strengthening effect has been compromised. This porous condition will be achieved by drilling shallow ½” diameter holes in the concrete surface to achieve a predetermined 5% or 10% loss in bonded area.

Goal of Experiment

From this experimental program, damage curves (see figure (4)) will be developed which can be used to determine the probable strength degradation of a CFRP strengthened concrete flexural member. These curves will be developed for the various sizes, locations, and types of defects that are tested. Additionally, this experimental program is being used for the development and verification of a finite element model to enhance our ability to assess defects on specimens of different geometry and material properties. The final goal of this experimental program is to verify and refine an analytical bond model that is currently under development for use in future design and analysis.

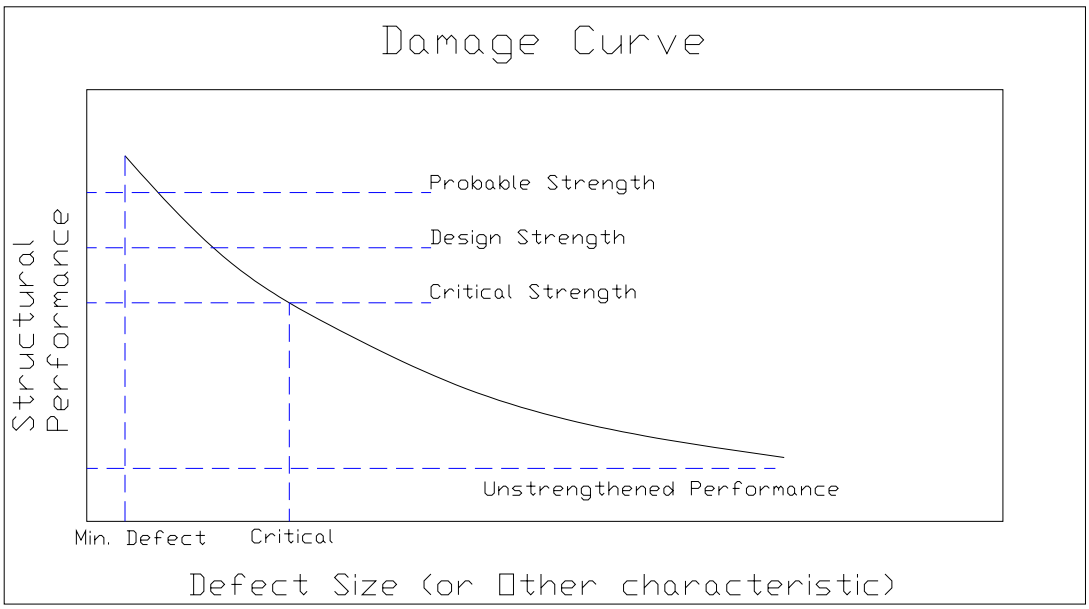

Figure 4: A primary goal of this research is to develop a damage curve to help assess defect criticality that is encountered in the field.

RESULTS

Table (1) summarizes the 30 tests conducted to date. Each specimen has been given a name based on defect type, location, and size. Four specimens were control specimens that were tested to failure without any FRP strengthening. Four are controls in which FRP was utilized, but no preload was applied and no defects were inserted. The last of the control specimens consisted of 5 tests where, like the specimens with defects, preload was utilized and FRP was applied, but obviously no defects were purposely inserted. Finally the specimens with defects are listed beginning with the specimens with the smallest defects and increasing in size down the list. Defect locations are given in millimeters distance from the midspan. Defect size is the defect diameter for circular specimens and length for the rectangular disbonds, also in millimeters. From the tests, it appears the shape of the defect is relatively unimportant. Instead, the determination of whether a defect is critical is more dependent on the defect length parallel to the fiber direction. This shape independence is because at loads significantly lower than those required for macro debonding, the stress concentrations in non-rectangular shapes cause local debonding to occur such that the defect then becomes simply a rectangular shaped debonded section, rather than the original shape.

Figure (5) shows a typical load vs. midspan displacement curve of an unstrengthened specimen, a strengthened specimen without a preload applied, and a strengthened specimen with preload applied. Point (a) is the initial cracking of concrete, points (b) is points of longitudinal steel yielding, points labeled (c) are debonding of the FRP and the corresponding total loss of strengthened performance. Note the increased stiffness due to FRP strengthening over the unstrengthened members. Also, notice the greater initial stiffness the precracked, strengthened specimens over those that were not precracked since the FRP may be activated earlier in a precracked member. Although the initial stiffness of a cracked, strengthened member appears to be slightly greater than an uncracked, strengthened member, the behavior seems to be virtually identical after sufficient load has been applied to each specimen to cause a large amount of additional cracking.

Table 1: Test Summary

Number of Tests	Test Description	Defect Location from midspan (mm)	Defect size (mm)	Defect Shape	Loading Description
4	Control (unstrengthened)	-	-	-	-
4	Control (No Preload, Strengthened)	-	-	-	-
5	Control (With Preload, Strengthened)	-	-	-	-
1	25C_185	185	25	Circular	High Moment, High Shear
1	25R_185	185	25	Rectangular	High Moment, High Shear
1	50C_185	185	50	Circular	High Moment, High Shear
1	50R_185	185	50	Rectangular	High Moment, High Shear
3	100C_185	185	100	Circular	High Moment, High Shear
1	100C_185E	660	100	Circular	Low Moment, High Shear
1	100C_428	428	100	Circular	Low Moment, High Shear
1	100C_0	0	100	Circular	High Moment, Zero Shear
2	100R_185	185	100	Rectangular	High Moment, High Shear
1	100R_0	0	100	Rectangular	High Moment, Zero Shear
2	150C_185	185	150	Circular	High Moment, High Shear
2	150R_185	185	150	Rectangular	High Moment, High Shear

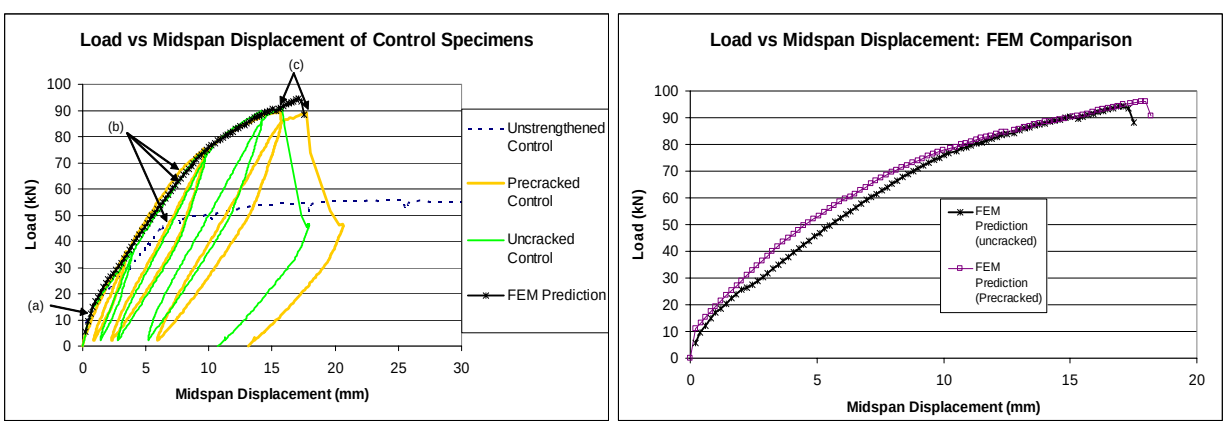

Figure 5: Applied load vs. midspan displacement of the three types of control specimens.

Figure (6) shows average load vs. midspan displacement plots with the load cycles removed for clarity. The plot includes average behavior for control specimens, specimens consisting of defects with dimensions smaller than 100mm, specimens with defects larger than 100mm, and

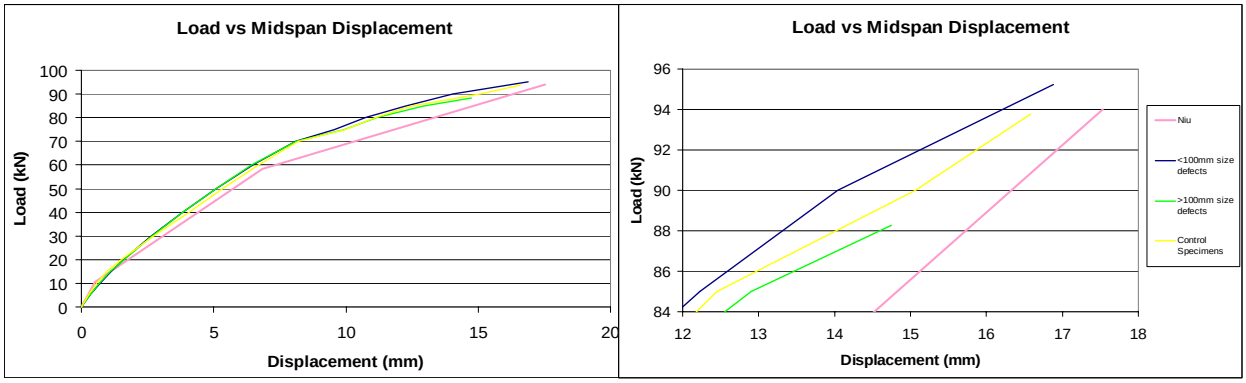

Figure 6: Applied load vs midspan displacement of specimens with different defect size characteristics.

finally the predicted results derived from the analytical bond behavior model currently under development. As can be seen from Figure (5), all the specimens exhibit very similar global behavior throughout the majority of the loading cycle. Specimens with disbond sizes smaller than 100mm or 6% of length of the FRP display virtually no change in global behavior. Also, maximum strength and displacement behavior is well predicted by the analytical bond behavior model. However, in the case of defects being 100mm or larger, noticeable strength and ductility loss is evident.

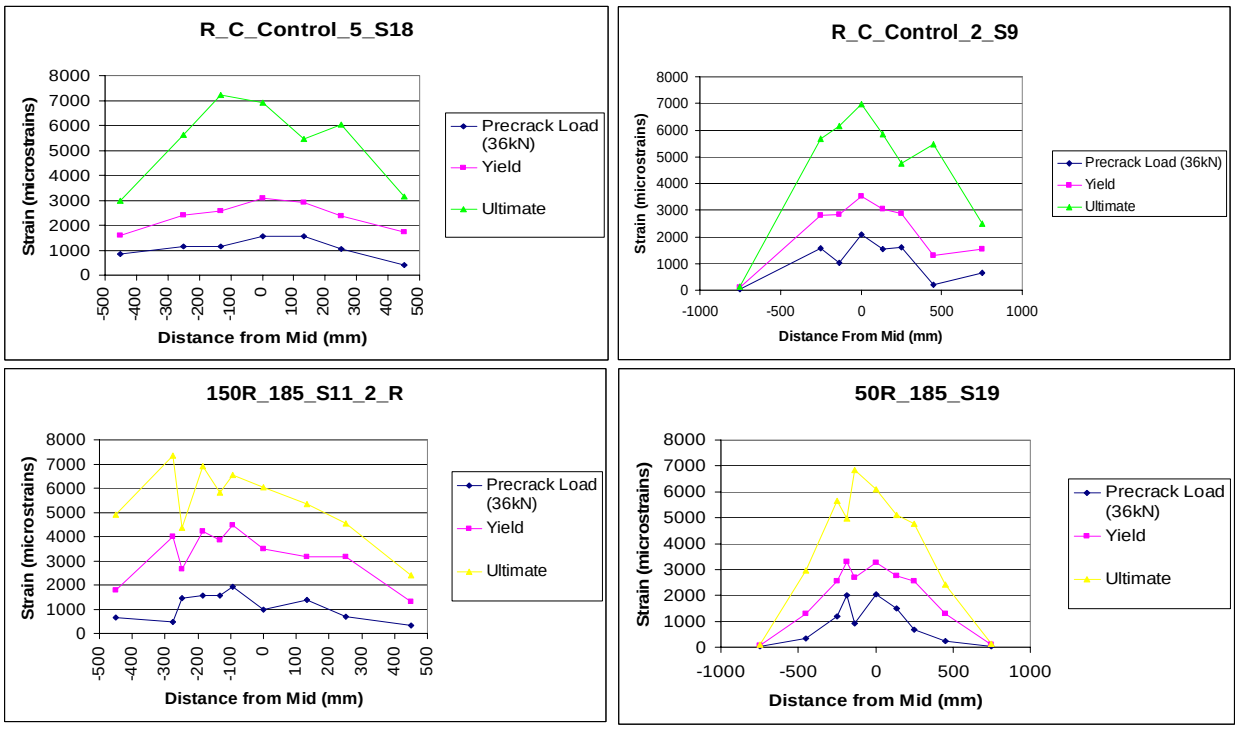

Figure 7: Strain development profiles at various load levels. Notice the peak strains for specimens with defects occur at the location of the defect, whereas the peak strains are near the midspan for control specimens.

Figure (7) shows the strain profile results obtained from the strain gages applied along the length of the FRP surface at three different load levels (Preload level, yield, and ultimate) for four different specimens. The top two specimens are both control specimens in which preload was applied before the application of FRP. The bottom left specimen consists of a 50mm rectangular defect, which is less than the critical size for global behavior degradation. The bottom right is a 150mm rectangular defect, which is larger than the described critical size. From these plots the local affect of a disbond is evident. The maximum (debonding) strain level for each of these specimens is near 7000 microstrains. For the two control specimens, this maximum strain for each load level is located, as expected, very near the midspan of the structure. For the specimens containing disbonds, however, the maximum strains are observed to be located at the location of the defect (185mm to the left of the midspan in these cases). Despite the 50mm defect being smaller than the critical size to observe a change in global performance, the performance can be observed to be quite different locally and could be useful information in future investigations involving durability.

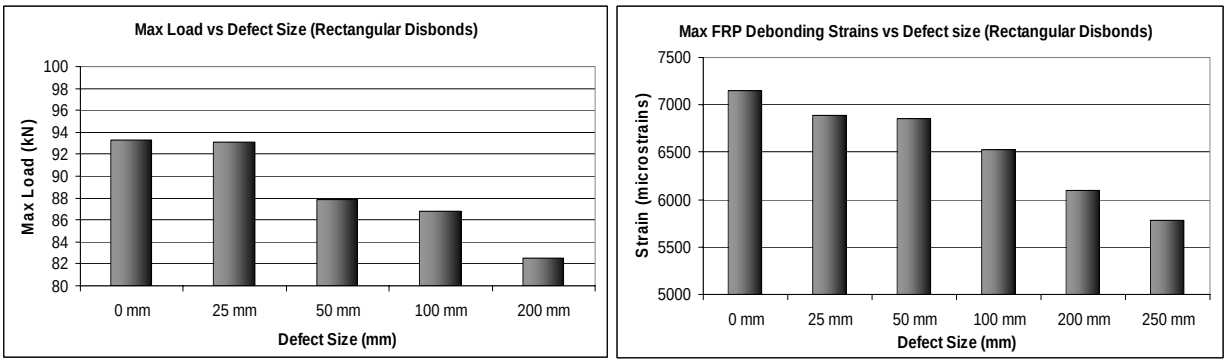

Figure 8: Preliminary results for maximum load and FRP debonding strains vs defect size

Figure (8) shows preliminary results for the maximum load and maximum FRP strain at debonding for several various disbond sizes. These rectangular defects start at zero millimeters and increase up to the very large dimension of 250mm in length. It is important to note the strength loss after the defect size is larger than 25mm and the loss in maximum FRP strain apparently due to stress concentrations and stiffness losses in the specimens containing a disbond.

CONCLUSIONS

From the results of this investigation it can be concluded that a critical defect size does appear to exist in which a disbond has very little impact on structural performance when it is smaller than this critical size. Fortunately, it appears the critical disbond size is quite large. In the case of this study the critical defect size is between 50mm and 100mm (3% and 6% of total FRP bond length respectively) in length parallel to the bonded length of FRP. In addition to the observation of a critical defect size, there also exist defect locations that are more critical than others. The most critical location appears to be in the region where the beam is experiencing both high moment and high shear about 185mm from the midspan. At this location, a large diagonal shear crack occurs in the strengthened beam, causing both mode I and mode II failure conditions to act at that location to initiate peeling of the FRP. It is therefore concluded that the cracking pattern in the concrete is extremely important to completely understand and model the behavior of a strengthened specimen. Numerical modeling has also demonstrated that an unbonded region at

the end of the FRP section has detrimental effects on strengthening performance. This is because the unbonded region at the end not only effectively shortens the length of the FRP section, but also induces a mode I peeling force normal to the concrete surface.

From this investigation, the relative effect of defects will be known and appropriate defect curves will be developed. Additionally, accurate analytical bond development and FEA models will be developed for future design and analysis projects and further investigation of defect criticality.

ACKNOWLEDGMENTS
The authors greatly appreciate the support of the California Department of Transportation and Fyfe Co. on this research project.

REFERENCES

1. ACI 440.2R-02, *Guide to the Design and Construction of Externally Bonded FRP Systems for Strengthening Concrete Structures*, American Concrete Institute, Framington Hills, MI, 2002.
2. Bizindavyi L. and Neale K.W., *Tranfer Lengths and Bond Strengths for Composites Bonded to Concrete*, ASCE Journal of Composites for Construction, Vol. 3 No. 4, p. 153, 1999.
3. Kaiser H., *Assessment of Defect Criticality and Non-destructive Monitoring of CFRP-rehabilitated Civil Structures*, Masters Thesis *Department of Structural Engineering*, UCSD: La Jolla, CA, 2002.
4. Navada R., *An Experimental Assessment of Defect Criticality in FRP Rehabilitated Concrete using a Fracture Mechanics Approach*, Mathers Thesis *Department of Structural Engineering*, UCSD: La Jolla, CA, 2004.
5. NCHRP Report 514 Transportation Researcher Board, Washington, D.C.
6. Niu H., Delaney J., Karbhari V., *Effect of Defects on Perforamnce of CFRP Strengthened RC Beams*, Sampe 2005 Long Beach Conference Procedings, 2005.
7. Ueda T., et. al., *Study on Behavior in Tension of Reinforced Concrete Members Strengthened by Carbon Fiber Sheet*, ASCE Journal of Composites for Construction, Vol. 6, No. 3, p. 168. 2002.
8. Yang X., Nanni A., Haug S., and Sun, C.L., *Strength and Modulus Degredation of CFRP Laminates from Fiber Misalignment*. Journal of Materials in Civil Engineering, American Society of Civil Engineers, Vol. 14, No. 4, pp. 320-326. 2002.